

Empirical density functional and the adsorption of organic molecules on Si(100)M. A. Phillips,¹ N. A. Besley,² P. M. W. Gill,² and P. Moriarty^{1,*}¹ School of Physics and Astronomy, The University of Nottingham, University Park, Nottingham NG7 2RD United Kingdom² School of Chemistry, The University of Nottingham, University Park, Nottingham NG7 2RD United Kingdom

(Received 18 May 2002; revised manuscript received 7 October 2002; published 15 January 2003)

Ab initio computational chemistry is finding increased use in the field of surface science, particularly in the study of adsorption. For semiconductor surfaces, such studies typically employ cluster models of the substrate. However, computational expense limits the cluster size and hence the type of adsorbate and range of adsorbate-substrate interactions that it is feasible to investigate. It is therefore desirable to obtain a calculation scheme which yields high accuracy for a minimum computational investment. Here the drawbacks of several approaches to this ideal are discussed, as are some general issues concerning the use of cluster models. In order to reduce computational expense to a level whereby the adsorption of large molecules (for example, fullerenes) may be studied, an empirical density functional, EDF1, has been applied in conjunction with the LANL2DZ pseudopotential basis set. The results of this calculation scheme are compared to those obtained using other functionals in conjunction with both all electron and the LANL2DZ pseudopotential basis sets. These results indicate that EDF1 can serve as a cost effective alternative to B3LYP.

DOI: 10.1103/PhysRevB.67.035309

PACS number(s): 68.43.Bc, 68.43.Fg

I. INTRODUCTION

Density-functional theory (DFT)¹ is now a well-established technique in computational chemistry, and is used by researchers working in many areas of physics, chemistry, and biochemistry. One area in which DFT has been exploited is in the study of adsorption processes; in particular, as interest in single-molecule devices has grown,²⁻⁴ DFT has been used to great effect to study the adsorption of organic molecules at surfaces. Given the recent developments in the manipulation of larger molecules, most notably fullerenes and nanotubes,⁵⁻¹⁰ there is particular interest in the theoretical study of their adsorption. However, as larger molecules are considered the number of calculations required for a complete investigation grows rapidly, due to the increase in number of possible binding configurations. Furthermore, it is necessary to consider a larger area of the substrate, which leads to a rapid increase in computational expense. For these reasons, if we wish to study the adsorption of large molecules, it is necessary to ensure that a computational scheme is used which yields high accuracy for an acceptably low computational investment.

Adsorption may be modeled through the use of either plane-wave calculations, which employ a supercell model of an area of surface, or calculations based on Gaussian basis sets, which use cluster models of the substrate. It is the accuracy of results as a function of computational expense in the latter case that is considered here, since this method has been used with some success to investigate the adsorption of small organic molecules—ethene, ethyne, cyclohexane and benzene, to name a few—at the Si(100) surface.¹¹⁻¹³

II. CLUSTER MODELS

Figure 1 shows a typical cluster model of the Si(100) surface. In this model, unfilled valencies on the peripheral “bulk” atoms are capped with hydrogen, while those at the (100) surface are left unsaturated so that they may dimerize.

In this way, the isolated clusters may be treated as charge neutral with singlet multiplicity in DFT calculations. Importantly, the cluster incorporates several layers of silicon, permitting the study of both the adsorption of a species onto the surface, and any resulting subsurface relaxations.

When studying adsorption at Si(100) with DFT in conjunction with cluster models, it is common to use clusters which contain one or two surface dimers. The use of clusters larger than this is rare, since the computational expense of a DFT calculation increases rapidly, typically as N^3 , where N is the number of basis functions. In order to consider larger adsorbates, or to investigate the long-ranged effects of adsorption, it is necessary to model a greater expanse of the substrate surface. Larger clusters have been used in this type of study, but some compromise between the level of theory and computational expense has been required. One such compromise is the use of *semiempirical* methods, such as the *Austin method 1* (AM1)¹⁴ or the *Parametrized method 3* (PM3).¹⁵ These semiempirical methods are much less computationally demanding than either Hartree Fock (HF) or DFT calculations, but this is achieved by neglecting many of the two-electron repulsion integrals, and approximating those that remain by a parametric form specific to the method in question. Parametrization of the model is completed through the fitting of various terms to experimental data. Historically, computational chemistry has been widely used in the study of organic systems, and so this parameter fitting is generally weighted so that the resulting semi-empirical algorithm yields excellent agreement with experimental data for organic species. As a consequence, such methods frequently give poor results for inorganic systems, and may therefore not be useful for the study of adsorption at semiconductor surfaces.

An alternative approach to the reduction of computational expense involves reducing the number of electrons in a system that must be treated using explicit quantum mechanics, and thus reducing the number of costly two-electron integrals that it is necessary to evaluate. It is possible to realize

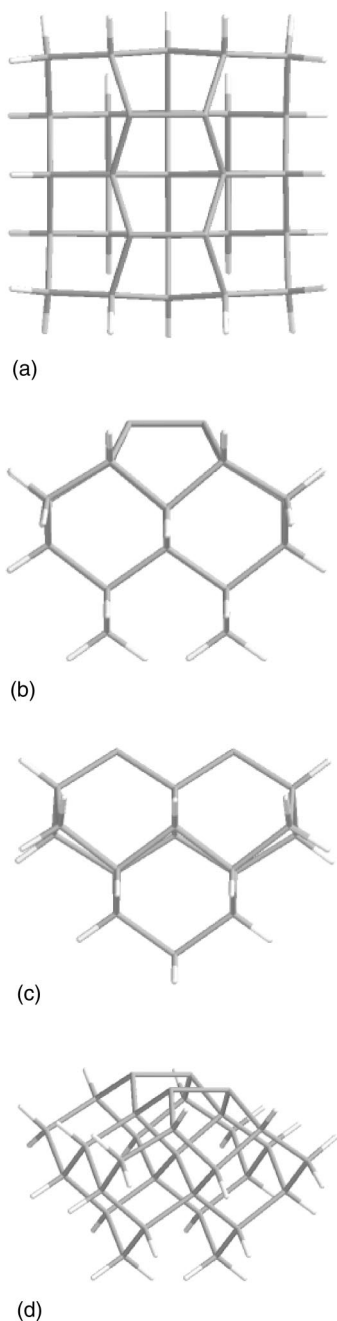


FIG. 1. A cluster model of the Si(100) surface viewed from above (a), the front (b), the side (c), and in perspective (d).

this through the use of a combination of quantum and classical mechanics in so-called Quantum mechanical/molecular mechanical (QM/MM) methods, as recently applied to Si(100) in pioneering studies by Gordon and co-workers^{16,17} In this method, the substrate model incorporates a large number of atoms, but most of these are treated using inexpensive molecular mechanics methods; only those which are involved in binding to the adsorbate, and some n nearest-neighbor atoms, are given a full quantum-mechanical treatment. One may also employ pseudopotential—or effective core potential (ECP)—basis sets to replace the core electrons of various atomic species with a function which represents

the effective potential due to these electrons. Clearly, the accuracy of results from a QM/MM method will be highly dependent on the quantum-mechanical scheme used. Furthermore, the development of a cost-effective quantum mechanical calculation scheme will benefit QM/MM methods, providing the potential to consider larger systems.

Pseudopotentials mimic the effects of core electrons on those in valence levels, which are considered explicitly using Gaussian functions, as in a standard basis set. However, the development of ECP basis sets has been driven by the need to reduce computational expense, and so the number of basis functions used to represent the remaining electrons is typically quite modest. Coupled with the fact that the majority of popular density functionals, for example B3LYP,^{18–20} generally give better results when used in conjunction with large basis sets, the performance of these functionals in conjunction with an ECP basis set can be poor, as will be illustrated.

III. EDF1

The starting point in the development of a density functional for computational chemistry is often the selection of a few exchange and correlation functionals which are based on models of particular physical situations. ‘Hybrid’ functionals, such as B3LYP, also include some contribution from the exact Fock exchange term from HF theory. The mixing coefficients of these components are then adjusted such that the results from the functional agree exactly with experiment for a particular system, or in some cases with the results from more complex theory applied to a small system.

In this spirit, the empirical density functional EDF1 was constructed²¹ by linearly combining a large number of widely used density functionals and the Fock orbital functional. Its mixing coefficients were varied to fit results from the functional to the G2 (Ref. 22) set of experimental data for small molecules, using the relatively small 6-31+G* basis set. In the fitting process, many mixing coefficients fell to zero, indicating that contributions from certain functionals are not beneficial within the limit of this basis set. Significantly, the exact Fock contribution is not required. Computationally, the Fock component is obtained through the analytical evaluation of electron-electron integrals. Exchange and correlation functionals, however, are evaluated using quadrature at points on a molecular grid. The absence of the exact Fock exchange in EDF1 eliminates the requirement for analytical evaluation of integrals: only the evaluation of integrals through numerical quadrature is required, and so it may be expected that the computational expense of EDF1 calculations will be lower than those carried out using hybrid functionals. Furthermore, EDF1 is optimized for use with a smaller basis set, and may hence be particularly suitable for use in conjunction with ECP basis sets.

IV. COMPUTATIONAL APPROACH

A. Cluster models

Cluster models of the semiconductor surface are popular in computational chemical investigations. Applied to the

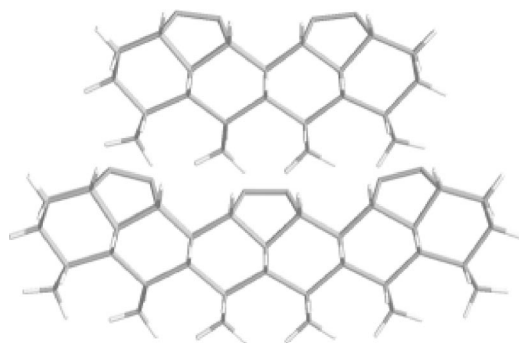


FIG. 2. Cluster curvature.

Si(100) surface, however, cluster models have drawbacks which are clearly apparent when larger areas of the surface are modelled, incorporating multiple dimer rows. Although less apparent in single-row clusters, the deficiencies of the cluster model may certainly affect results. The presence of dimer bonds on the upper surface of the cluster creates strain there and, in our preliminary investigations concerning multirow models, this was found to produce curvature of the cluster, as illustrated in Fig. 2, the radius of curvature decreasing as more dimer rows are considered. Clearly, the curved cluster is a poor model of the flat Si(100) surface, and some measure is required to minimize this curvature. This may be achieved by fixing the positions of some of the cluster's atoms. The question, then, is which atoms should be constrained and how their relative positions should be determined. We have considered several approaches to this problem.

The most self-consistent approach is, unfortunately, the most computationally expensive. A multirow cluster is extended to the maximum number of silicon layers possible, such that the last layer consists of a single silicon center, the two unfilled valencies of which are capped with hydrogen, yielding an *extended* cluster. This extended cluster is then used to represent the substrate in all subsequent calculations. Of course, the number of additional silicon layers that must be considered rises very rapidly with the number of dimers and dimer rows in the cluster. For any cluster larger than two rows containing two dimers each, the large computational expense renders this approach infeasible.

As an alternative, self consistency may be compromised to produce an approach which involves only one highly expensive step. The geometry of the extended cluster may be optimized at the same level of theory that will be used to calculate adsorption geometries, followed by the removal of excess silicon. The atoms of the lowest remaining layer are fixed in position and unfilled valencies are capped, giving a *cropped* cluster model. The cropped cluster is used for all subsequent calculations, both with and without adsorbates. Once again, however, this technique is not practical for clusters with more than two rows of two dimers.

It is possible to conceive of a further compromise, in which the extended cluster is optimized at a lower level of theory, but different levels of theory yield slightly different atomic coordinates in the lowest layer of the cropped cluster. The results from one method are not readily justified as more

appropriate as those from another and hence, in making this compromise, the self-consistency of this approach is lost, whilst the overall computational expense remains high. Finally, and importantly, for a fixed calculation scheme, the relative positions of atoms in the lowest layer of a cropped cluster can vary slightly, as more dimers or dimer rows are added. The extended-cropped cluster approach is therefore not desirable, either in terms of maintaining self-consistency in calculations or in reducing computational expense.

The approach used throughout this work is based on the observation that the lowest layer of atoms in the cluster model should be representative of bulklike silicon. For this reason, the position of atoms in this layer are obtained from considerations of the experimentally obtained lattice constant of bulk silicon, and its crystallographic structure. Unfilled valencies, with the exception of those on dimerising silicon centers, are capped with hydrogen atoms placed so that the H-Si bond lengths match the empirical H-Si bond length observed in SiH₄, and tetrahedral bond angles are preserved. Choosing the relative positions of silicon centres in this way is not theoretically self-consistent, but it removes the need for the costly optimization of an extended cluster and ensures that the structure of the "bulklike" layer does not vary with the number of dimers considered in the model. This *empirical* cluster approach is much more desirable as it incurs no additional computational expense, and maintains a degree of consistency amongst cluster models of varying size. It should be noted that QM/MM techniques also offer the possibility of preserving a level of self-consistency without geometric constraints, and we intend to apply this approach in a future investigation.

B. Calculation scheme

A large number of DFT calculation schemes have been considered, but we have concentrated on those achieved from combinations of the B3LYP or EDF1 functional with the all electron 6-31G* or LANL2DZ (Refs. 23 and 24) pseudopotential basis sets. For a particular calculation scheme and adsorbate in a specific binding configuration, binding geometry and energy were determined in the following way. The empirical cluster was optimized at the high level of theory, and the adsorbate manually constructed or placed in a position and orientation approximating the binding geometry of interest. A partial optimization of the bound system was then carried out at a low level of theory, AM1: all atoms within the system, with the exception of those constituting the adsorbate and the surface dimers it is bound to, are fixed in place permitting only the adsorbate and atoms at the binding site to relax to a closer approximation to the bound state. With only the lowest silicon atoms and lowest two layers of hydrogen atoms fixed in empirical positions once again, the system is optimized at the high level of theory, yielding the binding geometry and its absolute energy. This energy is used in conjunction with those from geometry optimizations of isolated cluster and adsorbate using the same calculation scheme to obtain the binding energy. All semiempirical calculations were performed using Wavefunction's *Spartan '02 for Linux*;²⁵ HF and DFT work was carried out using *Q-Chem 2.0*.²⁶

V. CLUSTER GEOMETRY

Experimentally, the Si-Si dimer bond is found to have a length of $2.24 \pm 0.08 \text{ \AA}$.²⁷ All of our geometry optimizations using combinations of the LSDA, B3LYP, and EDF1 density functionals with the 3-21G, 6-31G, 6-31G*, and LANL2DZ basis sets found the dimer length in the single-dimer cluster to be 2.23 \AA with a standard deviation of 0.02 \AA between calculation schemes and bond angles on the lowest Si species remaining close to a tetrahedral geometry. HF theory, when used with the same basis sets, generally permits a greater relaxation of bonds about the lowest Si atom, and returns shorter Si-Si dimer bond lengths; across basis sets, HF theory gives an average dimer length of 2.19 \AA with a standard deviation of 0.02 \AA .

Experimental data from scanning tunnelling microscopy (STM), photoemission spectroscopy,^{28,29} and x-ray diffraction³⁰ reveal that at room temperature the Si(100) surface dimers are not symmetric: they exhibit an anticorrelated buckling. However, dimer buckling is not fully understood theoretically, and predictions of the ground-state surface topography have been mixed:^{31–35} several groups have obtained results that indicate a buckled geometry, while others have found a symmetric dimer configuration to be energetically favorable. There is also clear evidence that slight changes in the physical constraints imposed on a cluster calculation can affect which configuration is favored.³⁶ In this investigation, all cluster models considered—standard (unconstrained), extended, cropped, and empirical—give results which favor the symmetric dimer configuration as the ground state at all levels of theory, despite much effort expended in attempts to reproduce dimer buckling through subtle variations in geometric constraints.

Given the controversy surrounding the buckled or unbuckled nature of the ground state, it is important to consider the effect of dimer buckling at nonzero temperatures (neglecting contributions from nonzero temperature vibrational states) on the binding energies and geometries obtained here. First, although the physical origins of dimer buckling are a subject of great debate, it is generally believed that the energetic difference between buckled and symmetric dimer states is small (0.1 eV) compared to adsorbate binding energies (2 eV).^{36,37} This error is of the same order or smaller than that inherent in the use of a density functional and an incomplete basis set. Should greater theoretical accuracy be required, however, it is possible that the energetic effects of dimer buckling may be included as a perturbation. Second, room-temperature STM images indicate that, upon the adsorption of a wide variety of molecular species, the dimers involved in adsorption drop out of the buckled state. From these considerations we are confident that, despite the widespread uncertainty concerning the Si(100) ground state geometry, the absence of dimer buckling observed here in the bare silicon cluster models is relatively insignificant when considering either binding geometries or binding energies, but may be important when considering adsorption pathways and the electronic structure of transition states.

VI. BINDING GEOMETRIES AND ENERGIES

Figure 3 shows some possible binding geometries for ethene and ethyne on single- and two-dimer clusters. It

should be noted that an additional stable state exists for ethyne on the two-dimer cluster, in which the adsorbate binds across two dimers. This state was not considered in this work, since the principal aim was to test the performance of EDF1 compared to B3LYP, and also that of the empirical clusters compared to other cluster models, studied extensively elsewhere. In all calculations for ethene and ethyne, there are no dangling bonds in the bound state; as such, all systems were treated as neutral singlets.

The single-dimer cluster is not subject to any geometric constraints. As such, its use ensures that calculations carried out elsewhere can be precisely reproduced and serves as an excellent system with which to compare different computational schemes. Table I shows the binding energies of ethene and ethyne to the single-dimer cluster obtained using HF and a number of DFT methods in conjunction with a variety of all electron Gaussian basis sets and the LANL2DZ pseudopotential basis.

It is important to note that the binding energies given in Table I have not been zero-point corrected: contributions to binding energy due to differences in the ground state vibrational energies of the isolated and bound systems have not been accounted for. Crude investigations with AM1 indicate that a correction of approximately -0.01 eV may be expected for each C-Si bond formed in the adsorption process, corresponding to the damping of the C-C stretch modes in the linear organic molecule. A more detailed study of zero-point corrections will be the subject of a subsequent investigation. The values obtained from B3LYP/6-31G* match those obtained by Konečný and Doren.¹²

Experimentally, temperature programmed desorption (TPD) techniques have shown the binding energies of ethene³⁸ and ethyne³⁹ to the Si(100) surface to be 1.65 and 2 eV , respectively. For both ethene and ethyne, EDF1 agrees better with these experimental results than HF or either of the other two density functionals when used with the same basis set. In the case of ethene, EDF1 agrees closely with experiment when used with any of these small basis sets, with the exception of the smallest, 3-21G. The same may not be said when considering ethyne, as all calculation schemes yield binding energies which are significantly larger than that obtained experimentally. However, it is important to realize that the accuracy of TPD techniques when used to determine binding energies varies with adsorbate, as discussed by Konečný and Doren.¹² Applied to ethene, TPD measurements may be expected to serve as an accurate probe of binding energy, since the majority of adsorbed molecules are desorbed. Ethyne, on the other hand, demonstrates a preference for thermal decomposition at the Si(100) surface: only a small proportion of adsorbed molecules are desorbed, and hence TPD may indicate a desorption energy which is significantly lower than that required to break Si-C bonds. This certainly appears to be the case.

Having compared various calculation schemes using the simplest possible cluster model, it is necessary to test the effectiveness of the empirical cluster model coupled with the LANL2DZ pseudopotential basis set applied to larger systems. Results from HF theory and the local spin density approximation (LSDA) functional are clearly inferior to those

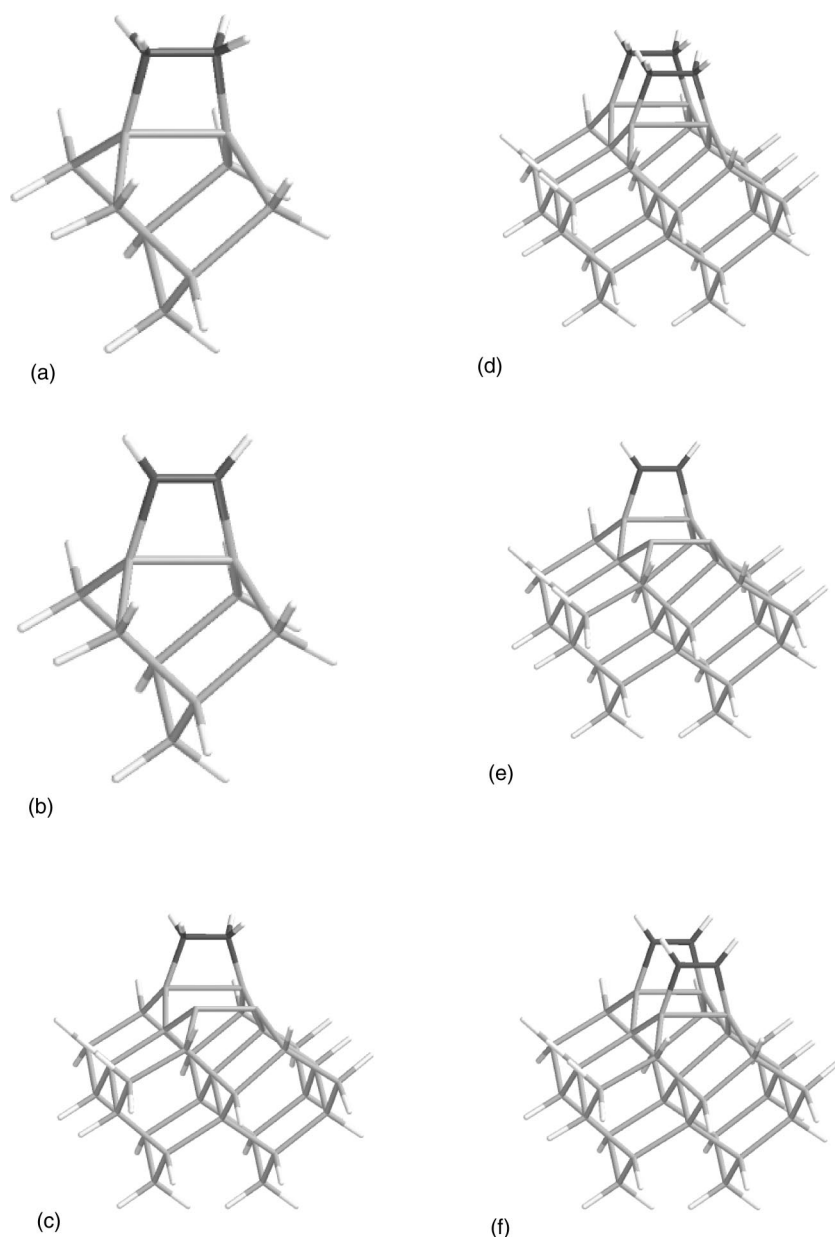


FIG. 3. Binding geometries for ethene [(a), (c) and (d)] and ethyne [(b), (e), and (f)] on single- and two-dimer clusters.

from either B3LYP or EDF1 even for the single-dimer cluster. Similarly, the 3-21G basis set appears to perform poorly. The LSDA functional, HF theory and 3-21G basis set were therefore not used when considering larger systems. Furthermore, despite its apparently inferior performance here, the 6-31G* basis set was chosen over 6-31G since it is a standard in computational chemistry and was used in the testing of various clusters. As such, four schemes of principal interest remain, comprised of the B3LYP and EDF1 functionals coupled with the all electron 6-31G* and pseudopotential LANL2DZ basis sets. Table II shows values of the binding energy of ethene to the two-dimer empirical cluster, obtained using these schemes.

Since many more silicon centres are present in the two-dimer cluster model, calculations with the all electron basis set are much more expensive than for the single-dimer cluster. For this reason, binding energies have been obtained with

TABLE I. Binding energies (in eV) of ethene and ethyne to a single-dimer cluster model, obtained using various functional/basis set combinations.

Ethene; experimental binding energy = 1.65 eV (Ref. 38).				
	HF	LSDA	B3LYP	EDF1
3-21G	2.41	3.02	2.25	2.05
6-31G	1.98	2.58	1.82	1.61
6-31G*	2.22	2.72	1.99	1.75
LANL2DZ	2.11	2.66	1.97	1.74
Ethyne; experimental binding energy = 2 eV (Ref. 39).				
	HF	LSDA	B3LYP	EDF1
3-21G	2.89	3.56	2.83	2.69
6-31G	2.63	3.24	2.53	2.38
6-31G*	3.04	3.54	2.86	2.68
LANL2DZ	2.75	3.32	2.67	2.49

TABLE II. Binding energy of ethene to a two-dimer empirical cluster, single (0.5 ML) and double (1 ML), obtained using B3LYP and EDF1 with both all electron and pseudopotential basis sets.

	Binding energy / eV			
	EDF1		B3LYP	
	6-31G*	LANL2DZ	6-31G*	LANL2DZ
single	1.86	1.85	2.13	2.37
double	1.78	1.75	2.07	2.30

all possible functional/basis set combinations only for ethene. In each case, it can be seen that there is a reduction in binding energy as the cluster coverage is increased from 0.5 ML to 1 ML (corresponding to single and double adsorption, respectively); indeed, this is to be expected as the energetic favorability of an adsorption event is certain to decrease as the number of available binding sites is decreased, in the absence of any attractive adsorbate-adsorbate interactions.

Once again, in all cases, EDF1 predicts adsorption energies which are closer to the experimentally determined value

of 1.65 eV than B3LYP. Importantly, there is only a small change in EDF1's adsorption energies when pseudopotentials are introduced. The same may not be said for B3LYP: as the number of basis functions is decreased, the performance of this functional is reduced, most likely because it is optimized for use with larger basis sets. For ethyne on the two-dimer empirical cluster, EDF1/LANL2DZ yields binding energies of 2.80 and 2.79 eV for single and double adsorption. Again, after consideration of the accuracy of thermal desorption measurements concerning ethyne on the Si(100) surface, these energies compare well with the experimental result of 2 eV. Binding energies for ethene obtained using EDF1/LANL2DZ of 1.85 eV (0.5 ML) and 1.75 (1 ML) compare more favorably with experiment than those obtained from periodic slab calculations carried out by Cho *et al.*⁴⁰ These slab calculations predict a buckled dimer geometry in the ground state, and yield binding energies of 1.89 and 1.93 eV for 0.5 and 1-ML coverages of ethene, and 2.74 and 2.72 eV for the same coverages of ethyne. It is clear, then, that empirical cluster models used in conjunction with EDF1/LANL2DZ achieve a comparable agreement with experi-

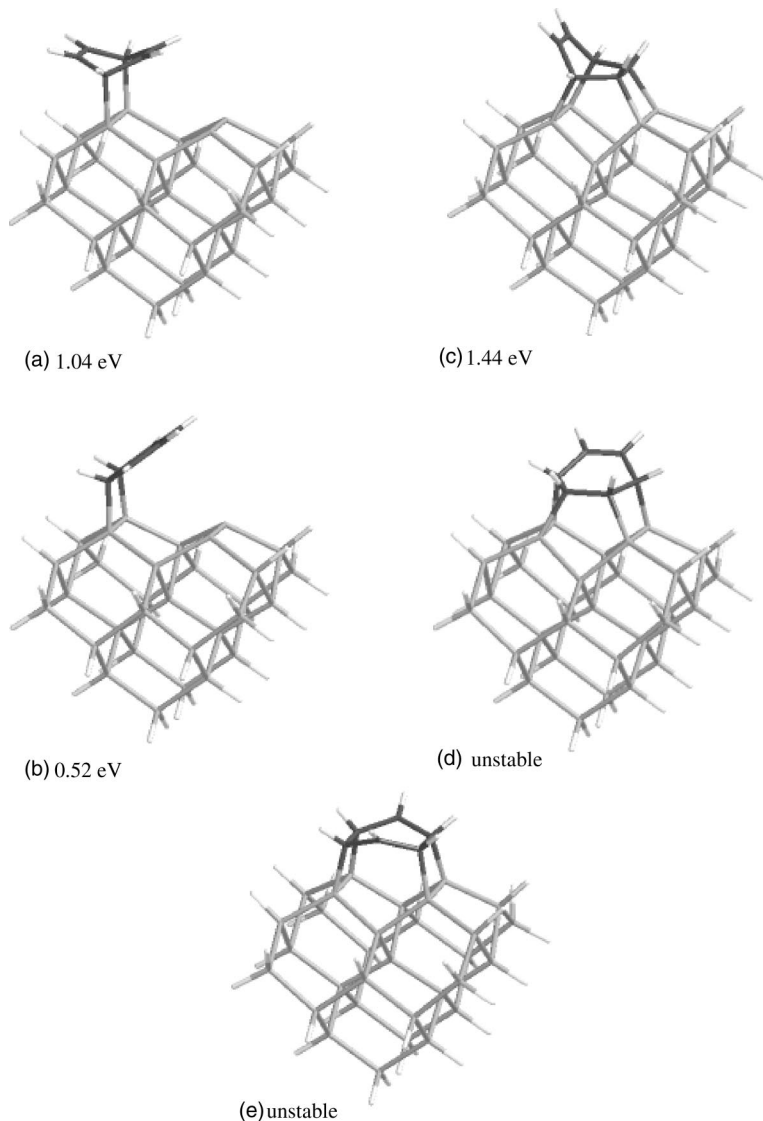


FIG. 4. Adsorption geometries of benzene on the Si(100) surface, with binding energies from EDF1/LANL2DZ.

TABLE III. Binding energies for stable states of benzene on Si(100)/eV.

	EDF1/LANL2DZ	B3LYP/6-31G* (Ref. 42)
Edge	0.52	n/a
1-4	1.04	1.04
Tight bridge	1.44	1.12

mental results, despite the absence of dimer buckling in the predicted ground state.⁴⁵ Calculations concerning ethene adsorbed on a cluster containing two rows of two dimers indicate a binding energy of 1.88 eV for 1 ML coverage.

The final test of the model concerns its performance when

considering larger adsorbates; benzene serves as a good test, since its adsorption on Si(100) has been studied extensively using both theoretical and experimental techniques. Figure 4 shows five possible adsorption geometries for benzene on Si(100). Using the nomenclature introduced by Wolkow *et al.*,⁴¹ these are termed (a) 1-4, or Diels-Alder configuration, (b) edge bound (c) the tight bridge (d) the twisted bridge, and (e) the symmetric bridge. The first four of these bound states were treated as neutral singlets. The symmetric bridge, however, has dangling bonds on the two C centers not involved in Si-C bond formation. For this reason, the symmetric bridge bound state was treated as a neutral triplet. EDF1/LANL2DZ indicates that of these five possible geometries, only three are stable. The binding energies for these

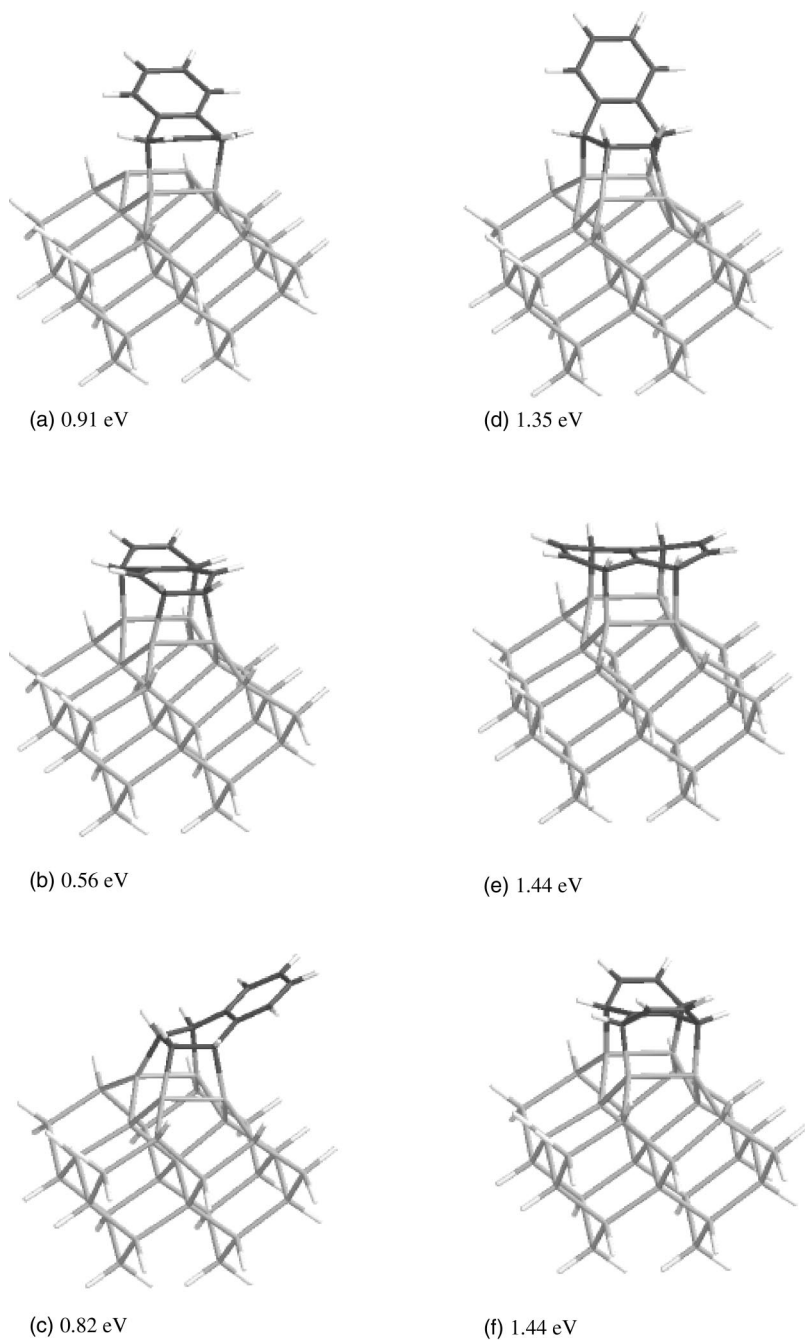


FIG. 5. Adsorption geometries of naphthalene on the Si(100) surface, with binding energies from EDF1/LANL2DZ.

TABLE IV. Vibration frequencies of the Si-H symmetric and antisymmetric stretch modes at the H-passivated Si(100) surface.

Mode	Frequency/cm ⁻¹		
	EDF1/LANL2DZ	B3LYP/LANL2DZ	Experimental (Ref. 44)
Symmetric	2174	2202	2097
Antisymmetric	2166	2201	2088

stable configurations are given in Table III, and compared to results obtained elsewhere using B3LYP/6-31G*.

Experimental TPD work⁴³ indicates two stable states at 1.21 and 1.39 eV. From the EDF1/LANL2DZ values, it is possible to assign the tight bridging and 1-4 configurations to the 1.39 and 1.21 eV states, respectively. EDF1/LANL2DZ predicts a small binding energy for the edge-bound state, which may be a metastable state occurring during desorption of tight bridged species.

Finally, we consider the prediction of binding energies and geometries for naphthalene at the Si(100) surface, using EDF1/LANL2DZ. Here, only binding geometries on top of a dimer row are considered, of which there are 15; the study of bound states between dimer rows would require the use of a four-dimer cluster, and will be the subject of subsequent work. Of the 15 possible bound states, only six were found to be stable. These are presented in Fig. 5 along with their binding energies, and we term them the (a) 1-4, or Diels-Alder, (b) medium-parallel, (c) tight-orthogonal, (d) tight-parallel, (e) symmetric-orthogonal, and (f) symmetric parallel configurations. Various spin states were considered, but all of the stable configurations shown here have singlet multiplicity and no excess charge. Analysis of C-C bond lengths reveals that rehybridization has taken place resulting in no unfilled valencies on any carbon centers. There are no experimental data available with which to compare these energies; however, the binding energy per Si-C bond formed is comparable to that obtained for the adsorption of ethene, acetylene and benzene, indicating that these results are not unreasonable.

VII. VIBRATIONAL SPECTRA

The symmetric and antisymmetric H-Si stretch frequencies at the hydrogen-terminated Si(100) surface have been determined experimentally with a high degree of confidence.⁴⁴ Table IV shows calculated harmonic frequen-

cies for these vibrational modes, obtained using both B3LYP and EDF1, in conjunction with the LANL2DZ pseudopotential basis set. Both the absolute values and the separation of the harmonic frequencies from EDF1/LANL2DZ match experimental results more closely than those from obtained from B3LYP/LANL2DZ.

VIII. CONCLUSIONS

The principal purpose of this investigation was the determination of a method by which the computational expense of DFT calculations could be reduced, without significant degradation in the results obtained. Pseudopotentials have long been used to achieve such a reduction, but when used with the popular B3LYP functionals the accuracy of results is compromised. Table V shows the relative processing times required for the evaluation of the self consistent field (SCF) and its gradients using combinations of B3LYP and EDF1 with 6-31G* and LANL2DZ for a number of systems. In terms of these computational times, at worst the performance of EDF1 is comparable to that of B3LYP for SCF evaluation. At best, there is a reduction in expense when using EDF1 compared to B3LYP, while results from the study of energetics indicate no significant loss in accuracy. Gradient evaluation times clearly show the benefit in terms of expense of the absence of Fock exchange in EDF1—the removal of the need to evaluate two-electron integrals is surely responsible for EDF1's cost effectiveness in this type of calculation when compared to B3LYP. It is also clear, in terms of both energetics and the SCF and gradient evaluation times, that EDF1 is more tolerant of the use of pseudopotentials, which can be seen to yield a much greater cost benefit when larger systems are considered.

With a significant reduction in computational expense, without sacrificing the accuracy of binding energies and vibrational structure data, EDF1 when coupled with pseudopotential basis sets is an attractive approach to the investigation

TABLE V. Relative computation times per optimization cycle for self-consistent field (SCF) and field gradient evaluations for various calculation schemes.

	Self-consistent field				Field gradients			
	B3LYP/ 6-31G*	EDF1/ 6-31G*	B3LYP/ LANL2DZ	EDF1/ LANL2DZ	B3LYP/ 6-31G*	EDF1/ 6-31G*	B3LYP/ LANL2DZ	EDF1/ LANL2DZ
One-dimer cluster	3.48	3.70	1.00	1.29	5.23	2.79	1.13	1.00
One-dimer cluster + C ₂ H ₂	3.07	2.84	1.01	1.00	5.09	2.51	1.15	1.00
One-dimer cluster + C ₂ H ₄	2.86	2.18	1.00	1.02	5.05	2.46	1.15	1.00
One-dimer cluster + 2H	7.88	5.49	1.20	1.00	11.75	3.86	1.52	1.00
Two-dimer cluster	11.45	2.79	1.20	1.00	23.51	2.13	1.62	1.00

of the adsorption of larger molecules in organic-silicon systems. Certainly, for the study of fullerenes, if long-range effects may be neglected, it may only be necessary to consider a two dimer by two row cluster model, which is certainly feasible with this calculation scheme. Additionally, since EDF1 has been shown elsewhere to perform well for short-range properties in a large variety of small systems, and here to provide excellent results in larger organic-silicon systems, this functional could be applied to great effect to similarly expensive calculations in other fields. Where longer-ranged effects may not be neglected, the performance demonstrated

here perhaps indicates that EDF1/LANL2DZ is a highly suitable calculation scheme for the quantum-mechanical portion of QM/MM calculations.

ACKNOWLEDGMENTS

Many thanks to Peter Beton for his invaluable input during a number of discussions. We are grateful to the Engineering and Physical Sciences Research Council for funding, in particular for a Joint Research Equipment Initiative grant for computing equipment.

*URL: <http://www.nottingham.ac.uk/physics/research/nano/>

- ¹P. Hohenberg and W. Kohn, *Phys. Rev.* **136**, B864 (1964).
- ²Y. Wada, *Proc. IEEE* **89**, 1147 (2001).
- ³H. W. C. Postma, M. de Jonge, Z. Yao, and C. Dekker, *Phys. Rev. B* **62**, R10 653 (2000).
- ⁴C. Joachim and J. K. Gimzewski, *Proc. IEEE* **86**, 184 (1998).
- ⁵P. Avouris, T. Hertel, R. Martel, T. Schmidt, H. R. Shea, and R. E. Walkup, *Appl. Surf. Sci.* **141**, 201 (1999).
- ⁶H. W. C. Postma, A. Sellmeijer, and C. Dekker, *Adv. Mater.* **12**, 1299 (2000).
- ⁷H. Tang, M. T. Cuberes, C. Joachim, and J. K. Gimzewski, *Surf. Sci.* **386**, 115 (1997).
- ⁸M. J. Butcher, F. H. Jones, P. Moriarty, P. H. Beton, K. Prassides, K. Kordatos, and N. Tagmatarchis, *Appl. Phys. Lett.* **75**, 1074 (1999).
- ⁹P. H. Beton, A. W. Dunn, and P. Moriarty, *Appl. Phys. Lett.* **67**, 1075 (1995).
- ¹⁰P. Moriarty, Y.-R. Ma, M. D. Upward, and P. H. Beton, *Surf. Sci.* **407**, 27 (1998).
- ¹¹W. Pan, T. Zhu, and W. Yang, *J. Chem. Phys.* **107**, 3981 (1997).
- ¹²R. Konečný and D. J. Doren, *Surf. Sci.* **417**, 169 (1998).
- ¹³W. A. Hoffer, A. J. Fisher, and R. A. Wolkow, *Surf. Sci.* **475**, 83 (2001).
- ¹⁴M. J. S. Dewar, E. G. Zoebisch, E. F. Healy, and J. J. P. Stewart, *J. Am. Chem. Soc.* **107**, 2902 (1985).
- ¹⁵J. J. P. Stewart, *J. Comput. Chem.* **10**, 209 (1989).
- ¹⁶Y. Jung, C. H. Choi, and M. S. Gordon, *J. Phys. Chem.* **105**, 4039 (2001).
- ¹⁷C. H. Choi, D.-J. Liu, J. W. Evans, and M. S. Gordon, *J. Am. Chem. Soc.* **124**, 8730 (2002).
- ¹⁸A. D. Becke, *J. Chem. Phys.* **98**, 5648 (1993).
- ¹⁹C. Lee, W. Yang, and R. G. Parr, *Phys. Rev. B* **37**, 785 (1998).
- ²⁰P. J. Stephens, C. F. Chablowski, and M. J. Frisch, *J. Chem. Phys.* **98**, 11623 (1994).
- ²¹R. D. Adamson, P. M. W. Gill, and J. A. Pople, *Chem. Phys. Lett.* **284**, 6 (1998).
- ²²L. A. Curtis, K. Raghavachari, G. W. Trucks, and J. A. Pople, *J. Chem. Phys.* **94**, 7221 (1991).
- ²³J. P. Hay and W. R. Wadt, *J. Chem. Phys.* **82**, 270 (1985).
- ²⁴W. R. Wadt and J. P. Hay, *J. Chem. Phys.* **82**, 284 (1985).
- ²⁵*Spartan '02 for Linux*, Wavefunction, Inc., 18401 Von Karman Avenue, Suite 370, Irvine, CA 92612 (2001).
- ²⁶J. Kong, *J. Comput. Chem.* **21**, 1532 (2000).
- ²⁷H. Over, J. Wasserfall, W. Ranke, C. Ambiatello, R. Sawitzki, D. Wolf, and W. Moritz, *Phys. Rev. B* **55**, 4731 (1997).
- ²⁸R. I. G. Uhrberg, E. Landemark, and Y.-C. Chao, *Surf. Sci.* **75**, 197 (1995).
- ²⁹T.-W. Pi, C.-P. Cheng, and I.-H. Hong, *Surf. Sci.* **418**, 113 (1998).
- ³⁰R. Felici, I. K. Robinson, C. Ottaviani, P. Imeratori, P. Eng, and P. Perfetti, *Surf. Sci.* **375**, 55 (1996).
- ³¹E. Penev, P. Kratzer, and M. Scheffler, *J. Chem. Phys.* **110**, 3986 (1999).
- ³²J. R. Shoemaker, L. W. Burggraf, and M. S. Gordon, *J. Chem. Phys.* **112**, 2994 (2000).
- ³³J. S. Hess and D. J. Doren, *J. Chem. Phys.* **113**, 9353 (2000).
- ³⁴M. S. Gordon, J. R. Shoemaker, and L. W. Burggraf, *J. Chem. Phys.* **113**, 9355 (2000).
- ³⁵O. Paz, A. J. R. da Silva, J. J. Saenz, and E. Artacho, *Surf. Sci.* **482-485**, 458 (2001).
- ³⁶C. Yang and H. C. Kang, *J. Chem. Phys.* **110**, 11 029 (1999).
- ³⁷S. B. Healy, C. Filippi, P. Kratzer, E. Penev, and M. Scheffler, *Phys. Rev. Lett.* **87**, 016105 (2001).
- ³⁸L. Clemen, R. M. Wallace, P. A. Taylor, M. J. Dresser, W. J. Choyke, W. H. Weinberg, and J. T. Y. Jr, *Surf. Sci.* **268**, 205 (1992).
- ³⁹P. A. Taylor, R. M. Wallace, C. C. Cheng, W. H. Weinberg, M. J. Dresser, W. J. Choyke, and J. T. Y. Jr, *J. Am. Chem. Soc.* **114**, 6754 (1992).
- ⁴⁰J.-H. Cho, L. Kleinman, C. T. Chan, and K. S. Kim, *Phys. Rev. B* **63**, 073306 (2001).
- ⁴¹R. A. Wolkow, G. P. Lopinski, and D. J. Moffat, *Surf. Sci.* **416**, L1107 (1998).
- ⁴²W. A. Hofer, A. J. Fisher, G. P. Lopinski, and R. A. Wolkow, *Phys. Rev. B* **63**, 085314 (2001).
- ⁴³Y. Taguchi, M. Fujisawa, T. Takaoka, T. Okada, and M. Nishijima, *J. Chem. Phys.* **95**, 6870 (1991).
- ⁴⁴M. Niwano, M. Terashi, and J. Kuge, *Surf. Sci.* **420**, 6 (1999).
- ⁴⁵Following the suggestion of a referee, in order to compare the accuracy of the density-functional techniques considered here to a higher level of theory, we have carried out coupled cluster (CCSD) calculations on organic-silicon systems involving a single-dimer cluster model of the substrate. Unfortunately, these computationally expensive calculations did not conclusively demonstrate the superiority of either B3LYP or EDF1 in terms of the accuracy of the results.